

Creation and measurement of long-lived magnetic monopole currents in spin ice

S. R. Giblin^{1*}, S. T. Bramwell^{2*}, P. C. W. Holdsworth³, D. Prabhakaran⁴ and I. Terry⁵

The recent discovery of ‘magnetricity’ in spin ice raises the question of whether long-lived currents of magnetic ‘monopoles’ can be created and manipulated by applying magnetic fields. Here we show that they can. By applying a magnetic-field pulse to a Dy₂Ti₂O₇ spin-ice crystal at 0.36 K, we create a relaxing magnetic current that lasts for several minutes. We measure the current by means of the electromotive force it induces in a solenoid coupled to a sensitive amplifier, and quantitatively describe it using a chemical kinetic model of point-like charges obeying the Onsager-Wien mechanism of carrier dissociation and recombination. We thus derive the microscopic parameters of monopole motion in spin ice and identify the distinct roles of free and bound magnetic charges. Our results illustrate a basic capacitor effect for magnetic charge and should pave the way for the design and realization of ‘magnetronic’ circuitry.

Since the early pioneering work of Debye, Hückel, Bjerrum and Onsager on model electrolytes, the physics of Coulombic systems has been elucidated in many contexts, from electrolytes to dusty plasmas^{1,2}. These systems show a rich phenomenology and share many universal properties, which arise from the long-ranged and algebraic nature of the Coulomb interaction. A recent addition to this class is spin ice, where emergent magnetic monopoles form a magnetic Coulomb gas, and in which monopole currents have been detected.

Spin-ice materials such as Ho₂Ti₂O₇ and Dy₂Ti₂O₇ are ‘frustrated ferromagnets’ that form a disordered low-temperature magnetic state^{3–5}, in which the configurations of atomic magnetic moments or spins map onto proton configurations in water ice. On the basis of a well-established microscopic description⁶, it was proposed that thermally excited point defects in the spin-ice state take the form of magnetic charges or ‘monopoles’⁷ (see also refs 8,9). Subsequent work found consistency with this picture^{10–14}. In ref. 11 we argued that spin ice should conduct charge like a weak electrolyte (‘magnetolyte’¹⁵) and showed that Onsager’s theory of the field dissociation or Wien effect in weak electrolytes¹⁶ applies to spin ice. We used this to demonstrate the existence of magnetic currents and to measure the ‘elementary’ magnetic charge $\pm Q \approx 4.6 \mu_B \text{ \AA}^{-1}$ (ref. 11).

The model is of free (f) charges in dynamical equilibrium with bound (b) charge pairs according to the reaction scheme:

$$\phi = [\oplus\ominus]_b = \oplus_f + \ominus_f \quad (1)$$

where ϕ is the quasiparticle vacuum. According to the Onsager theory, the application of a magnetic field affects only the forward reaction of the right-hand equilibrium: it increases the rate of pair dissociation but not of recombination, so the (chemical) equilibrium constant is increased. That is, the chemical equilibrium, equation (1), is pushed to the right, and the system is forced out of thermodynamic equilibrium, into a steady state, so that the linear increase in the charge-carrier density with field, $\Delta n_f(B)$, is

an explicitly non-equilibrium effect. The free-charge density per Dy ion at equilibrium, or in steady state, $n_f^{\text{eq}} = n_f^{\text{eq}+} = n_f^{\text{eq}-}$, and the consequent conductivity κ , depend on field as:

$$\frac{n_f^{\text{eq}}(B)}{n_f^{\text{eq}}(0)} = \frac{\kappa(B)}{\kappa(0)} = 1 + \frac{b}{2} + \frac{b^2}{24} + \dots \quad (2)$$

where b is the dimensionless group $b = \mu_0 Q^3 B / 8\pi k^2 T^2$. Equation (2) is generally valid in the limit where the association is almost complete: $n_b^{\text{eq}} \gg n_f^{\text{eq}}$, but also applies for all $n_b^{\text{eq}}/n_f^{\text{eq}}$ if the left-hand equilibrium relaxes on a sufficiently fast timescale^{16,17}. In this case, the vacuum acts as a buffer, ensuring that on applying a field, n_b^{eq} remains unchanged.

This description of a magnetic property by an equation of electrolyte theory is a further universal consequence of the Coulomb interaction: it implies that many electrical effects will have their counterpart in magnetic systems. In this context, an elementary property is the response of the current to an abrupt change in external conditions, as typified by the discharge of a capacitor. Therefore, a principal aim of the present experiment was to study the evolution of magnetic current following the removal of a magnetic field. Naively, this should result in the decay of both a free current, arising from the unbound charges, and a polarization current, arising from the bound pairs, so that there should be two relaxation processes. This is exactly what we observe at $T = 0.36$ K in our experimental data, shown below.

The total magnetic current density is equal to the rate of change of magnetization $-\partial \mathbf{M} / \partial t$, which is proportional to the measured electromotive force. The relaxing magnetization \mathbf{M} is very different from that of a conventional magnet, as the magnetic charge $-\nabla \cdot \mathbf{M}$ is quantized, point-like (to a good approximation) and deconfined, and the magnetic current results from a flux of these point-like Coulombic charges. Although the current is transient, the charges have a finite mobility in exact analogy with ions in an electrolyte. Our data may thus be analysed to confirm the Wien dissociation and to derive quantitative microscopic information about reaction rates and mechanisms. In this sense our experiment is equivalent

¹ISIS Facility, Rutherford Appleton Laboratory, Chilton, OX11 0QX, UK, ²London Centre for Nanotechnology and Department of Physics and Astronomy, University College London, 17–19 Gordon Street, London, WC1H 0AH, UK, ³Université de Lyon, Laboratoire de Physique, École Normale Supérieure de Lyon, 46 Allée d’Italie, 69364 Lyon Cedex 07, France, ⁴Department of Physics, Clarendon Laboratory, University of Oxford, Park Road, Oxford, OX1 3PU, UK, ⁵Department of Physics, University of Durham, Durham, DH1 3LE, UK. *e-mail: sean.giblin@stfc.ac.uk; s.t.bramwell@ucl.ac.uk.

to those pioneered by Eigen and collaborators¹⁸ on the analogous electrical systems, whereby the relaxation of the Wien dissociation, following an electrical field pulse, was used to determine the kinetics of ionic association. The protocol is also reminiscent of those used to probe non-equilibrium phenomena in glassy systems¹⁹.

The precision measurement of magnetic relaxation in spin ice poses special challenges, owing to the low temperatures and small magnetic fields involved, and the extremely small changes in induction to be measured. We used a sensitive low-field measurement technique previously developed by two of us²⁰. A field $B \equiv \mu_0 H$ was applied to the sample for time t_0 and abruptly removed at the start of the measurement, time $t = 0$ (note that henceforth B represents the applied field). A solenoid attached to a superconducting quantum interference device (SQUID) susceptometer was used to measure the relaxation of magnetic moment density $\mu(t)$ (see the Methods section).

Model for the magnetic relaxation

In basic electrolyte theory, and its application to spin ice, there are several important length scales. These include the Bjerrum length²¹, $l_T = \mu_0 Q^2 / 8\pi kT$, which distinguishes free from bound charges; the Debye length $l_D = ((\mu_0 Q^2 2c_f) / kT)^{-1/2}$, which determines the effective range of the Coulomb interaction (here, c_f is the free-charge concentration); the field length $l_B = kT / QB$, and the lattice constant, or effective ionic diameter a . The interplay of these length scales, as a function of field and temperature, determines the essential properties of the system. In spin ice, the monopoles populate a diamond lattice with near-neighbour distance $a = 4.3 \text{ \AA}$; for convenience, we also define a length scale $a' = 2.50 \text{ \AA}$, which is the magnitude of the projection of the corresponding vector \mathbf{a} onto $[100]$, the field direction used in the present study. The monopole charge is $Q = 4.266 \times 10^{-13} \text{ JT}^{-1} \text{ m}^{-1}$ and the best numerical estimate for the chemical potential in the ‘spin-ice Coulomb gas’^{7,10}, constructed from the dipolar spin-ice model⁶, is $v_f/k_B = -4.45 \text{ K}$ (ref. 22). The length scales l_T , l_D and l_B are fully determined by these parameters.

Neglecting screening, the linear Wien effect reflects the relative magnitude of l_T and l_B . At a charge separation $r > l_T$, the thermal energy kT is sufficient to overcome the Coulomb interaction, $\mu_0 Q^2 / 4\pi r$ (ref. 16), whereas for $r < l_B$ free diffusive motion of monopoles remains possible. The universal dimensionless number of Onsager’s theory is simply the ratio $b = l_T / l_B$. In analogy with electrolytes²³, we expect that the density of bound and free charges at a distance r from a test charge of opposite sign placed at the origin should be maximal at the nearest-neighbour distance a and the association distance l_T , respectively. This is because the pair distribution function decreases monotonically with distance along any given direction (Fig. 1).

The Debye screening can be neglected in the formation of bound pairs as long as the Debye length is greater than the Bjerrum length, which is the case at low temperature. For $T > 1 \text{ K}$, l_D is very short, only exceeding two lattice spacings for $T < 0.9 \text{ K}$. At $T \approx 0.65 \text{ K}$, which marks the onset of slow dynamics²⁴, l_D becomes greater than l_T , rapidly becoming very long at lower temperatures, which allows for a clear separation of length scales, $l_D \gg l_T \gg a$. This condition of length-scale separation is achieved only at the lowest temperature used in the present study, $T = 0.36 \text{ K}$, where we have $l_D \approx 200 \text{ \AA}$, $l_T = 18.3 \text{ \AA}$, $a = 4.3 \text{ \AA}$.

The neglect of screening is strictly valid only if $l_D > l_B$; otherwise a modified theory involving l_D is applicable^{25,26}. This condition is not satisfied for the very small field values used in our experiments; for example $l_B = 1,100 \text{ \AA}$ at $B = 0.0001 \text{ T}$ and $T = 0.36 \text{ K}$, yet the unscreened Wien effect (equation (2)) accurately describes our data and l_D does not seem to be a relevant length scale. It is possible that on larger timescales than those studied here, one could observe a crossover to the modified theory in which l_D appears.

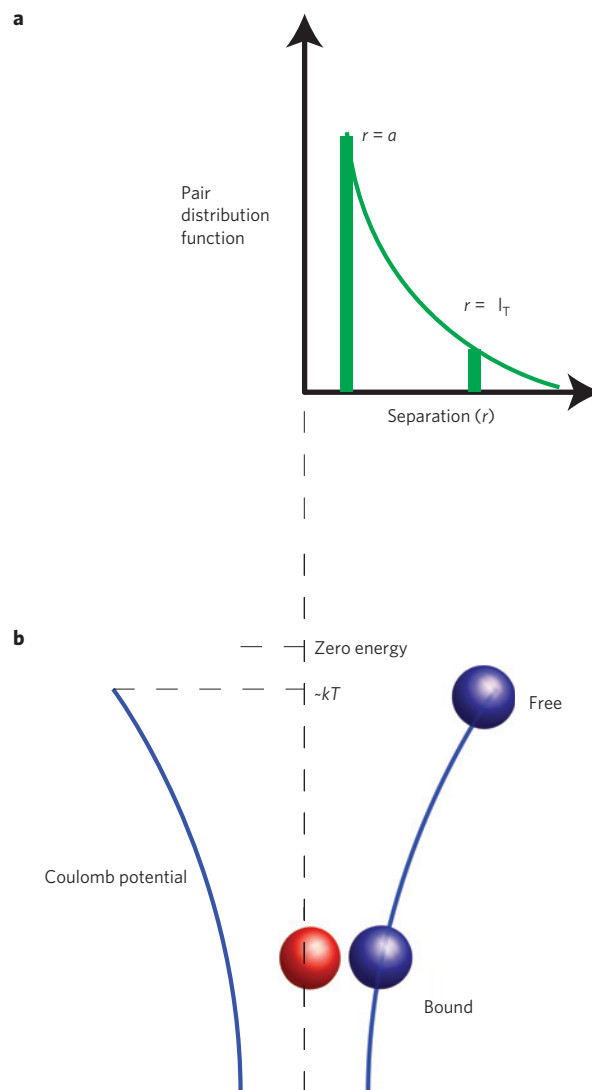


Figure 1 | Distance dependence of magnetic monopole interactions in spin ice. Charges of opposite sign are bound in pairs by the Coulomb potential ($\sim 1/r$) if their separation r is less than the association distance $r = l_T$. **a**, Pair distribution function $n(r)$. The density of bound pairs, at distance r along a chosen axis, is maximal at their shortest possible separation, $r = a$ (an effective hard-core repulsion), whereas that of free charges is maximal at $r = l_T$, just outside the association volume (vertical thick green lines). **b**, Thermal fluctuations liberate the charges from their mutual Coulomb interaction and so produce free charges in a narrow energy band of width $\sim kT$ near to zero energy.

The magnetic moment density, μ , may be considered to be made up of contributions from bound and free monopoles, $\mu = \mu_b + \mu_f$. We make the assumption, justified *a posteriori*, that any perturbation away from the true equilibrium of zero field is sufficiently small for the system to be treated with chemical thermodynamics. From here we have derived (see the Methods section) a relationship between μ_f and the field-induced change in free-particle concentration through the change in Wien equilibrium:

$$\mu_f^{\text{eq}}(B) = (Ql_T) \Delta n_f^{\text{eq}}(B) \quad (3)$$

The superscript eq denotes equilibrium or steady-state quantities: n_f^{eq} is the free-charge concentration in zero field and $n_f^{\text{eq}} + \Delta n_f^{\text{eq}}(B)$ is its steady-state value in applied field B . Equation (3) is a striking

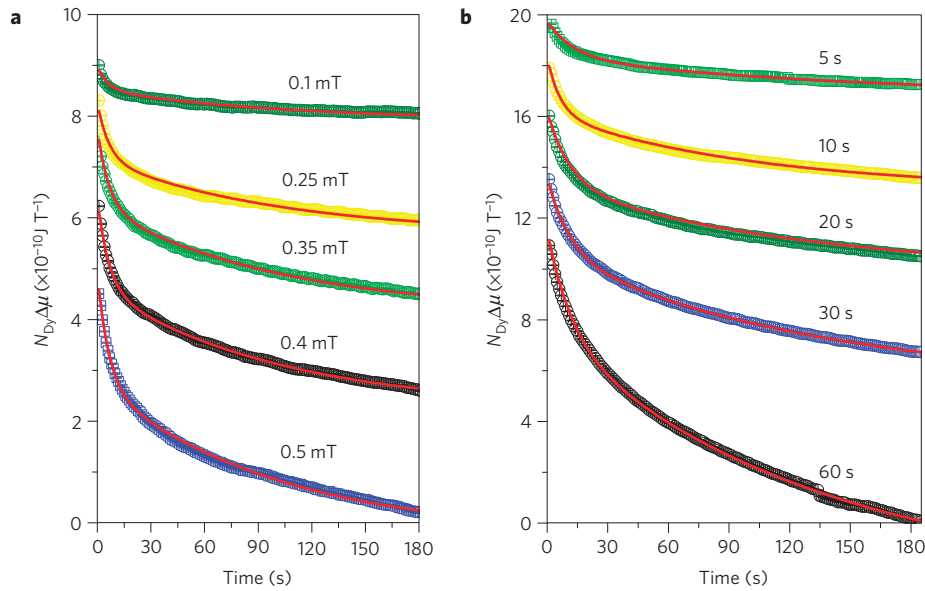


Figure 2 | An effective capacitor discharge for magnetic monopoles in spin ice. Observed magnetic moment change for various experimental conditions compared to the prediction of a chemical kinetic model of charge generation and dissociation (red lines) of magnetic monopole currents. The graphs show the measured magnetic moment $N_{Dy} \Delta\mu(t)$ of a crystal of spin ice, $Dy_2Ti_2O_7$, following the application and removal of a field (B , applied along the $[100]$ crystallographic axis) for a finite period of time (t_0). Here, N_{Dy} is the number of Dy ions in the sample and μ is the magnetic moment density per Dy ion. **a**, 10-s field pulses of varying magnitude. **b**, Fixed-amplitude (0.5 mT) pulses of varying duration. The curves are offset for clarity. Using the chemical kinetic model described in the text, the data have been fitted to produce parameters $k_{Or} = 0.099 \pm 0.009 \text{ s}^{-1}$, $k_D = 0.000134 \pm 0.00001 \text{ s}^{-1}$, $T_b = 3.33 \pm 0.05 \text{ K}$, $T_f = 4.52 \pm 0.10 \text{ K}$ (here, quoted standard errors are computed from the best-fit parameters for the nine data sets). Note that, although $\Delta\mu(t)$ is measured on an absolute scale, the measuring technique does not locate its zero, which has therefore been fitted as a parameter for each curve. The experimental resolution is smaller than the symbol size.

result, as it shows that all pairs that unbind as a result of the presence of the field are oriented along the field direction and that they contribute to the total moment as if separated by the escape distance l_T , even in the steady state. The form of the pair distribution function for free charges ensures that unbound charges seem to accumulate in correlated dipoles of moment Ql_T (Fig. 1b). Furthermore, using equation (2) it follows that the Wien effect can be rewritten to lowest order in field in an experimentally accessible form:

$$\mu_f^{\text{eq}}(B) = \frac{1}{2}(Ql_T)bn_f^{\text{eq}} \quad (4)$$

This formalism predicts a linear magnetic response at low temperature, which is quite different from that of a conventional Ising ferromagnet, or a cooperative paramagnet such as the nearest-neighbour model for spin ice. In the former, one expects a gapped excitation spectrum and an exponentially small magnetic response, whereas for the latter one expects a modified Curie law²². Here we have a gapped response, as $n_f(T)$ falls exponentially to zero at low temperature, but the effective moments are composite dipoles of moment Ql_T , scaled up from the magnetic moments on the dysprosium ions by a factor (l_T/a). This is a combined effect of the deconfinement of the magnetic monopoles and the appearance of l_T as the natural length scale over which charge inhomogeneities develop.

In addition to the free particles, the bound pairs will also contribute to the response to the perturbing field B : the bound-pair concentration does not change to first order in the field, but the field-induced reorientation or polarization of bound pairs will produce a magnetic moment μ_b that is linear with the field, analogous to the dielectric response of a polar fluid. This moment is the thermal average of the contributions of dipole moments of magnitude $\sim Qr$ between $r = a$ and $r = l_T$ (see Fig. 1). We introduce $\Delta\tilde{n}_b = [n_b \cos(\theta)]$, where θ is the angle made by a bound pair with

the field direction and where [...] is the configurational average over all pairs. In steady state $\Delta\tilde{n}_b^{\text{eq}} = n_b^{\text{eq}} \langle \cos(\theta) \rangle$, where $\langle \dots \rangle$ is a thermal average. In the Methods section, we argue that, as most pairs are separated by distances close to the nearest-neighbour distance, the moment arising from reoriented bound pairs is, to within a factor of order unity:

$$\mu_b^{\text{eq}}(B) = (Qa')\Delta\tilde{n}_b^{\text{eq}} \quad (5)$$

where

$$\Delta\tilde{n}_b^{\text{eq}} \approx (Qa'B/kT)n_b^{\text{eq}} \quad (6)$$

The moments μ_f^{eq} (equation (3)) and μ_b^{eq} (equation (5)) are steady-state contributions to the total magnetic moment. Their independent relaxation would give rise to two exponential decays. However, they are not independent: $\Delta\tilde{n}_b(t)$ is fuelled by the rebinding of free charges from the excess $\Delta n_f(t)$. As excess free particles are aligned with the field, such a recombination process changes both the bound-particle concentration and the orientation anisotropy of the bound pairs. Similarly, as there is a build up of orientated bound pairs, if there is further dissociation of pairs this process will be weighted in favour of orientated pairs. We therefore propose that the two species are connected by the chemical equilibria of equation (1), from which we deduce the following linearized rate equations:

$$\frac{d\Delta n_f(t)}{dt} = k_D \Delta\tilde{n}_b(t) - 2K^{-1}k_D n_f^{\text{eq}} \Delta n_f(t) \quad (7)$$

$$\frac{d\Delta\tilde{n}_b(t)}{dt} = -(k_{Or} + k_D) \Delta\tilde{n}_b(t) + 2K^{-1}k_D n_f^{\text{eq}} \Delta n_f(t) \quad (8)$$

Here k_{Or} is the rate constant for orientation of dipoles, which we expect to be a rapid process with its scale fixed by creation and

annihilation of bound pairs from the vacuum; k_D is the rate constant for dissociation of bound charges, which we expect to be slow in comparison; $K = (n_f^{eq})^2/n_b^{eq}$ is the equilibrium constant of the dissociation–recombination reaction.

Using the equilibrium values as boundary conditions, the total magnetic moment $\mu(t) = \mu_b(t) + \mu_f(t)$ was calculated, starting at $t = -t_0$, by numerically solving the linearized rate equations to first order in field with dynamic variables $\mu_b(t)$ and $\mu_f(t)$ given by expressions equivalent to equations (3)–(6).

Experimental test of the kinetic model

Our experimental data revealed a two-timescale, approximately exponential, decay that was particularly distinct at $T = 0.36$ K and 0.55 K, at short ‘charging’ times t_0 , but essentially merged into a single-exponential relaxation by $T = 0.7$ K. By $T = 1$ K, no relaxation was observed, indicating that all response had become too rapid to be observed in the experimental time window. At $T = 0.36$ K, the timescale of the faster relaxation was about 10 s, and that of the slower one was several hundred seconds.

At $T = 0.36$ K, experimental relaxation data sets $\Delta\mu(t)$ were collected for nine combinations of field-pulse parameters $\{t_0, B\}$. We found that these nine data sets could be fitted to the numerical solution of equations (7) and (8) using, within experimental error, a single set of parameters $\{k_D, k_{Or}, n_b^{eq} \equiv e^{-T_b/T}, n_f^{eq} \equiv e^{-T_f/T}\}$. The result is shown in Fig. 2, where one can see that the kinetic model clearly provides an excellent description of the experimental data at $T = 0.36$ K, giving strong support to our physical interpretation of the observed relaxation. The coupling of the relaxations of free and bound charge is necessary to produce fits of this quality. To confirm this, we compared the kinetic model with the alternative model, which has two exponential contributions relaxing independently: $\Delta\mu = \sum_i \mu_i(T_i) e^{-\nu_i t} (1 - e^{-\nu_i t_0})$ (here $i = b, f$). Each data set was fitted independently by the two models and the average best parameters for each model were used to generate relaxation curves. In contrast to the kinetic model, the two-exponential fit fails to describe the t_0 -dependent data: that is, there is no single set of parameters that can describe the whole experimental data set (Fig. 3b).

The parameter $T_f = 4.52 \pm 0.10$ K extracted from the experiment is approximately the free-charge creation energy. It implies a chemical potential in the spin-ice Coulomb gas of $\nu_f = 4.7(1)$ K (because $\exp(-T_f/T) = (1/2)\exp(-\nu_f/T)$), in excellent agreement with the numerical estimate, 4.45 K (ref. 22). The rate constant $k_R = K^{-1}k_D = 1.04 \times 10^3 \text{ s}^{-1}$ is that for free-charge recombination, and may be used to estimate a hopping frequency for magnetic monopoles, $1.8 \times 10^3 \text{ s}^{-1}$, (see Table 1 and the Methods section). This estimate is consistent with the relaxation frequency deduced from high-temperature a.c.-susceptibility $\tau^{-1} \sim 10^3 \text{ s}^{-1}$, and is close to the muon relaxation rate at 0.35 K ($\sim 10^4 \text{ s}^{-1}$; ref. 11). Thus, as far as the free charges are concerned, our results are in excellent agreement with expectations based on theory and other experiments. Furthermore, the timescale $(2n_f k_R)^{-1}$ may be simply interpreted as the monopole lifetime, which we identify as about 150 s at $T = 0.36$ K. It should be noted that whereas the rate of monopole hopping $\sim k_R$ is relatively fast, the rate of recombination $k_R n_f^2$ is extremely slow, as recombination events are relatively rare: such behaviour is akin to an electrolyte, where ionic recombination is many orders of magnitude slower than local ionic motion.

The second temperature scale extracted from the experiment, $T_b = 3.33 \pm 0.05$ K, is particularly notable, as it is considerably less than the energy, $\Delta E \approx -2\nu_f + V(a) = 5.83$ K, necessary to produce a nearest-neighbour bound pair of monopoles in the low-temperature limit for the spin-ice Coulomb gas²². To make an accurate estimate for the bound-pair concentration, one needs to take into account the basin of attraction offered by the long-range Coulomb interaction, which renormalizes this energy scale by an association coefficient. The dominant contribution comes from

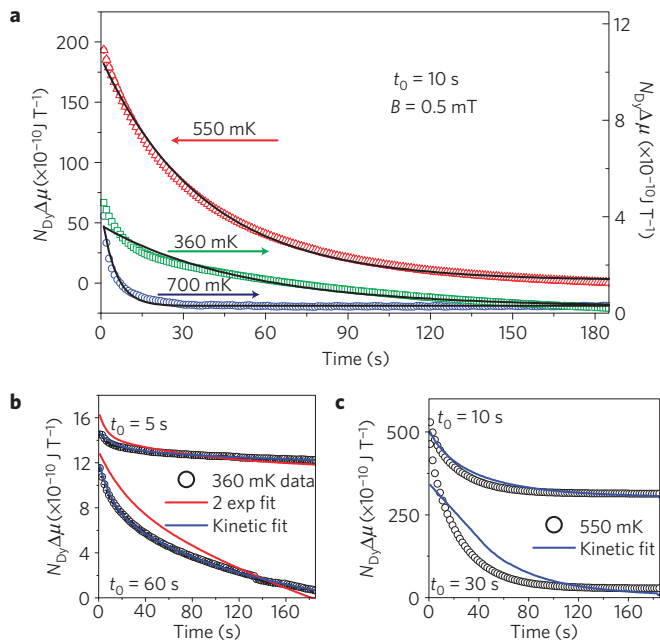


Figure 3 | Demonstration of the requirement for the chemical kinetic model at $T = 360$ mK and its breakdown at higher temperature.

a, Temperature-dependent magnetic relaxation measured in this work, with single-exponential fits to the data (black lines): the single-exponential description, although reasonable at higher temperature, breaks down at 360 mK. **b**, The full data set at 360 mK can be fitted by a single set of parameters using the kinetic model, but not using a model of two independent exponential relaxations (the figure shows two representative fits). **c**, As the temperature is raised to 0.55 K the data cannot be fitted to a single set of parameters, even using the kinetic model. All data shown have an applied field of 0.5 mT with the temperature and charging time (t_0) shown on each graph.

the four nearest-neighbour sites¹⁶, so that the energy scale is reduced to $T_b^{eff} \sim 5$ K, which is still considerably larger than the 3.33 K estimated experimentally and larger than T_f , which fixes the free-particle density.

Thus, the experimental T_b implies that $n_b \gg n_f$, which is the opposite limit to the dipolar spin-ice model. Although the validity of the Wien formula does not depend on this, the coupled kinetics of two competing phenomena and the substantial decay of $\mu(t)$ at short timescales are convincingly modelled with a high concentration of bound pairs. The large bound-pair concentration deduced from the experiment could be due to non-equilibrium effects: as observed numerically in thermal quenches²⁷, the kinetic constraints imposed by the classical ‘Dirac strings’ connecting the particles in the spin-ice Coulomb gas ensure that monopole pairs are often unable to annihilate and are blocked in deep metastable states at low temperature. Furthermore, the measured rate of their reorientation (0.07 s^{-1}) is surprisingly slow, as one might have expected it to be closer to the hopping rate of $2 \times 10^3 \text{ s}^{-1}$, and the slow rate seems compatible with the existence of such states. The discrepancy could also come from corrections to spin-ice Coulomb gas physics, such as the small bandwidth expected for the Pauling states⁶, the inclusion of further neighbour exchange interactions²⁸ or from small impurity concentrations.

At $T = 0.55$ and 0.7 K, the above arguments, based on well-separated length scales, l_D , l_T and a , break down. This is consistent with the measured data, which could not be fitted to the kinetic model at $T > 0.36$ K. Figure 3a illustrates data as a function of temperature for identical conditions ($t_0 = 10$ s, $B = 0.0005$ T). In the time window of the experiment, the response

Table 1 | Estimated parameters at $T = 0.36$ K.

Description	Symbol	Measured	Expected
Dissociation rate constant	k_D	$1.3(1) \times 10^{-4} \text{ s}^{-1}$	
Recombination rate constant	k_R	$1.04 \times 10^3 \text{ s}^{-1}$	
Pair-orientation rate constant	k_{Or}	$9.9(9) \times 10^{-2} \text{ s}^{-1}$	
Mean monopole hop rate	$\sim ck_R(a/l_T); c \approx 7.7$	$1.8 \times 10^3 \text{ s}^{-1}$	$\sim 10^3 \text{ s}^{-1}$ (refs 10,24)
Mean monopole lifetime	$\sim (2k_R n_f)^{-1}$	$\sim 150 \text{ s}$	
Dissociation equilibrium constant	$K = k_D/k_R = n_f^2/n_b$	1.25×10^{-7}	
Bound-pair density per Dy	$n_b = e^{-T_b/T}$	$1.0(1) \times 10^{-4}$	$\sim 10^{-6}$ (this work)
Free-charge density per Dy	$n_f = e^{-T_f/T}$	$4(1) \times 10^{-6}$	2×10^{-6} (ref. 10)

Single standard-deviation errors on directly estimated quantities are given in brackets.

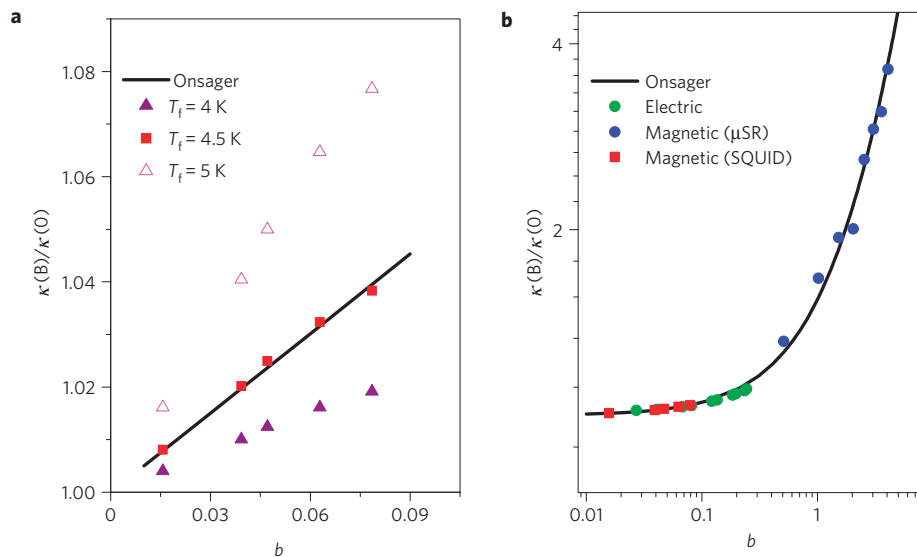


Figure 4 | A near-perfect symmetry between electricity and magnetism illustrated by data collapse onto Onsager's universal curve for the Wien effect¹⁶.

a, Results of the present experiment as a function of the Onsager dimensionless field b represented by plotting the quantity $\kappa(B)/\kappa(0) = 1 + \mu_i^{\text{eq}}/Ql_T n_f$, where μ_i^{eq} is extrapolated from the measured magnetic relaxation data, and $n_f = e^{-T_f/T}$, with T_f close to the free-charge chemical potential $v_f/k_B \approx -4.5$ K given by theory²² (sensitivity of the fit to T_f is illustrated). **b**, Our data (red squares) on logarithmic scales, compared to the relative electrical conductivity of acetic acid at $T = 298$ K (ref. 31; green circles) and relative muon relaxation rate of spin ice¹¹ at $T = 0.1$ K (there are no fitting parameters).

is peaked at $T = 0.55$ K, indicating a crossover in behaviour around this temperature, as previously observed²⁴. Moreover, Fig. 3c demonstrates that the kinetic model cannot describe the $T = 0.55$ K data with a single set of parameters.

The tendency to a single-exponential decay at higher temperature agrees with previous observations²⁴ and is evidence that the system crosses over to a fully dissociated but strongly screened Coulomb gas¹⁰ that exhibits only a free-current contribution to $\mu(t)$. The description of spin ice as a weak magnetolyte thus seems to be valid at $T < 0.5$ K. In the crossover regime between weak magnetolyte and strong magnetolyte, bulk measurements reveal various degrees of dynamical freezing in $\text{Dy}_2\text{Ti}_2\text{O}_7$ between 0.7 and 0.3 K (refs 24,29,30). Our results provide evidence that these non-equilibrium phenomena are direct consequences of the analogy with weak electrolytes: the linear increase in free-charge density leads to a linear magnetic response that can be accounted for only through non-equilibrium physics¹⁶.

Universal data collapse

The present experimental data may be used to make a stringent test of the Wien effect, which is almost independent of any interpretation attached to the kinetic fits of Fig. 2. The steady-state moment $\mu_i^{\text{eq}}(B)$ at $T = 0.36$ K can be estimated from the fits to equations (7) and (8) as the asymptotic value of μ_f at large time.

It can then be used to test equation (4), which is directly derived from the Wien effect, by plotting $1 + \mu_i^{\text{eq}}/Ql_T n_f$ versus the Onsager dimensionless parameter b , where we expect data collapse onto the function $f(b) = 1 + b/2 + b^2/12 + \dots$ (equation (2)). Here, n_f may either be considered a fitting parameter or else fixed to the theoretical value, $n_f = (1/2)\exp(v_f/k_B T)$, using the numerical estimate for the chemical potential, $v_f/k_B = -4.45$ K (ref. 22). The result is shown in Fig. 4a, where it can be seen that there is excellent agreement with the Onsager prediction, indicating that the phenomenology presented here and in ref. 11 is correct. In particular, the unequivocal appearance of the Bjerrum length, l_T , as the length scale on which charge inhomogeneities appear in the experiment is very strong evidence that important particle–particle correlations occur in the spin-ice Coulomb gas and that it is the Coulomb interaction that sets the scale for them.

A more comprehensive data collapse onto Onsager's universal curve is illustrated in Fig. 4b, which plots the relative muon relaxation rate of spin ice¹¹ and the relative electrical conductivity of acetic acid as reported by Gledhill and Patterson³¹, as well as the points extracted from the present data and analysis. The collapse of data over a broad range of experimental systems, techniques and parameter ranges is very striking and unequivocally demonstrates the universal applicability of Onsager's result to both electricity and magnetism.

In the spirit of this equivalence, the present experiment may also be interpreted as a demonstration of a capacitor effect for magnetic charges in spin ice. Excess charge is stored in the spin-ice sample under the action of an applied potential, which may be released on a slow timescale by removal of the potential. In the future it will be interesting to see if other basic ‘magnetronic’ effects can be similarly identified, which may be combined to make a functional device.

At a more fundamental level, we have demonstrated how, at low temperatures, spin ice behaves very differently from an idealized polarizable fluid or paramagnet, which would exhibit an exponential relaxation with a single, fast timescale, or from a spin glass that has a hierarchy of decays^{19,32}. In spin ice the basic rate in the system—the monopole hop rate—is always relatively fast, whereas the bulk relaxation is relatively slow, on account of the diminishing monopole population. The key length scales in the system, l_D and l_T , diverge only at zero temperature, so under no realizable conditions is there a truly divergent timescale.

Our results finally illustrate a tractable solution to a non-equilibrium dynamical many-body problem of great complexity. It may be relevant to solving other problems in the non-equilibrium behaviour of spin ice²⁷, that of other exotic magnets^{33–35} and artificial spin-ice systems^{36–38}. The spin-ice monopole system seems to be a practical example of a nearly ideal Coulomb lattice gas with perfectly symmetric charges that are confined to the sample. It might therefore give a useful new angle on the rich and subtle physics of the analogous electrical system^{23,39} and Coulomb fluids in general¹.

Methods

Equation (3) is derived as follows (see also ref. 11). At constant temperature, the total differential of the Gibbs energy for the dissociation equilibrium is $dG = -\mu_b^{\text{eq}}dn_b - \mathcal{A}d\xi$, where $\xi = n_f$ is the extent of reaction and $\mathcal{A} = kT \ln K - kT \ln(n_f^2/n_b)$ is the affinity (assuming activity coefficients are unity). It follows that $(\partial \mu_b^{\text{eq}}/\partial n_b)_B = (\partial \mathcal{A}/\partial B)_{n_f} = kT(\partial \ln K/\partial B)_{n_f} = kTb/B = Ql_T$ to leading order in b (using Onsager’s formula, equation (2) main text). Integration of this equation gives equation (3). In principle the above analysis is valid only at equilibrium, but assuming linear response theory to hold then the above expression should be applicable to the kinetic terms in equations (7) and (8) (main text).

Equations (5), (6) are defined as follows. The structured monopole vacuum is made up of ionic magnetic moments or spins, μ_{Dy} (ref. 15). A single spin flip creates a bound pair of charges with an emergent dipole moment of magnitude $Qa = 2\mu_{Dy}$. The spins can be divided into two classes, where flipping out of the vacuum creates a monopole pair oriented either with or against the field. Considering only nearest-neighbour pairs and working to first order in monopole concentration, the partition function for an N moment vacuum plus excitations can be written: $Z = [1 + \exp(-T_b/T) \exp(2\beta\mu_z B)]^N [1 + \exp(-T_b/T) \exp(-2\beta\mu_z B)]^N$, where $\mu_z = \mu_{Dy}/\sqrt{3}$ is the projection of the moment along the field axis and where T_b represents the effective single-spin-flip energy scale once the effect of long-range interactions has been taken into account. Defining the average magnetic moment density from bound charges as $\mu_b^{\text{eq}} = -(1/N)\partial G/\partial B$, where G is the magnetic Gibbs free energy, one finds $\mu_b^{\text{eq}} = -2\mu_z \delta n_b$, where δn_b is the contribution to $\Delta \bar{n}_b^{\text{eq}}$ coming from nearest-neighbour bound pairs. Expanding to first order in magnetic field and noting that $n_b^{\text{eq}} = \exp(-T_b/T)$, one finds the Curie law result for emergent bound-pair dipoles, $\delta n_b = (2\mu_z B/kT)n_b^{\text{eq}}$. Inserting the magnetic charge and approximating δn_b by $\Delta \bar{n}_b^{\text{eq}}$, we arrive at equations (5), (6).

The $Dy_2Ti_2O_7$ crystal used in these experiments was grown at Oxford University using an optical floating-zone furnace⁴⁰. The mass of the sample was 33 mg and it was cut approximately in a cuboid with dimensions $3 \times 1.5 \times 1.5$ mm. The sample used here was not used in previous experiments¹¹. Bulk magnetic measurements were carried out at Durham University using an Oxford Instruments Helium 3 system modified to include a quantum design d.c. SQUID with a first-order gradiometer pickup coil configuration, which enabled moment changes of 1×10^{-12} J T⁻¹ to be detected²⁰. Our experiment involved zero-field cooling the crystal and applying a field $B = \mu_0 H$ along the [100] crystallographic axis. The ramping rate was directly observed using an oscilloscope with both the charging and discharging time taking 0.5 s. The electromotive force induced in a solenoid with eight turns was converted to a potential by a SQUID device that integrated the signal to return changes in flux $\Delta \Phi(t)$. These were expressed, through a calibration procedure, as changes in sample moment $\Delta \mu(t)$. As a result of the integration, each data set (i) had an unknown offset $\Delta \mu_0(i)$ that needed to be treated as an unknown parameter in the data analysis.

The expression for monopole hopping rate ν_0 quoted in Table 1 was derived as follows. We approximate the diffusion constant $D = (1/6)a^2\nu_0$ and write the

mobility $u = DQ/kT$. Using Onsager’s analysis¹⁶, our recombination rate may be written $k_R = 8\pi kT(u/Q)l_T/V_{Dy}$, where V_{Dy} is the volume per dysprosium ion. These equations may be solved to give the quoted result.

Received 16 June 2010; accepted 25 November 2010;
published online 13 February 2011

References

- Bonitz, M., Henning, C. & Block, D. Complex plasmas: A laboratory for strong correlations. *Rep. Prog. Phys.* **73**, 066501 (2010).
- Hansen, J. P. & McDonald, I. R. *Theory of Simple Liquids* (Academic, 1986).
- Harris, M. J., Bramwell, S. T., McMorrow, D. F., Zeiske, T. & Godfrey, K. W. Geometrical frustration in the ferromagnetic pyrochlore $Ho_2Ti_2O_7$. *Phys. Rev. Lett.* **79**, 2554–2557 (1997).
- Bramwell, S. T. & Gingras, M. J. P. Spin ice state in frustrated magnetic pyrochlore materials. *Science* **294**, 1495–1501 (2001).
- Ramirez, A. P., Hayashi, A., Cava, R. J., Siddharthan, R. B. & Shastry, S. Zero-point entropy in spin ice. *Nature* **399**, 333–335 (1999).
- Melko, R. G. & Gingras, M. J. P. Monte Carlo studies of the dipolar spin ice model. *J. Phys. Condens. Matter* **16**, R1277–R1319 (2004).
- Castelnovo, C., Moessner, R. & Sondhi, S. L. Magnetic monopoles in spin ice. *Nature* **451**, 42–45 (2008).
- Ryzhkin, I. A. Magnetic relaxation in rare-earth pyrochlores. *J. Exp. Theor. Phys.* **101**, 481–486 (2005).
- Nussinov, Z., Batista, C. D., Normad, B. & Trugman, S. A. High-dimensional fractionalization and spinon deconfinement in pyrochlore antiferromagnets. *Phys. Rev. B* **75**, 094411 (2007).
- Jaubert, L. D. C. & Holdsworth, P. C. W. Signature of magnetic monopole and Dirac string dynamics in spin ice. *Nature Phys.* **5**, 258–261 (2009).
- Bramwell, S. T. *et al.* Measurement of the charge and current of magnetic monopoles in spin ice. *Nature* **461**, 956–959 (2009).
- Fennell, T. *et al.* Magnetic Coulomb phase in the spin ice $Ho_2Ti_2O_7$. *Science* **326**, 415–417 (2009).
- Morris, D. J. P. *et al.* Dirac strings and magnetic monopoles in the spin ice $Dy_2Ti_2O_7$. *Science* **326**, 411–414 (2009).
- Kadowaki, H. *et al.* Observation of magnetic monopoles in spin ice. *J. Phys. Soc. Jpn* **78**, 103706 (2009).
- Castelnovo, C. Coulomb physics in spin ice: From magnetic monopoles to magnetic currents. *Chem. Phys. Phys. Chem.* **11**, 557–559 (2010).
- Onsager, L. Deviations from Ohm’s law in weak electrolytes. *J. Chem. Phys.* **2**, 599–615 (1934).
- Pearson, R. G. Rates of ion recombination in solution by a radio-frequency dispersion method. *Discuss. Faraday Soc.* **17**, 187–193 (1954).
- Eigen, M. & Demeyer, L. Self-dissociation and protonic charge transport in water and ice. *Proc. R. Soc. Lond. A* **247**, 505–533 (1958).
- Bouchaud, J. P., Cugliandolo, L. F., Kurchan, J. & Mézard, M. in *Spin Glasses and Random Fields* Vol 12 (ed. Young, A. P.) (World Scientific, 1998).
- Read, D., Giblin, S. R. & Terry, I. Low temperature magnetic susceptometer based upon a d.c. superconducting quantum interference device. *Rev. Sci. Instrum.* **77**, 103906 (2006).
- Bjerrum, N. Untersuchungen über Ionenassoziation. *Kgl. Danske Vidensk. Selsk., Math.-fys. Medd.* **7**, 1–48 (1926).
- Jaubert, L. D. C. *Topological Constraints and Defects in Spin Ice*. PhD thesis, École Normale Supérieure de Lyon (2009).
- Camp, P. J. & Patey, G. N. Ion association in model ionic fluids. *Phys. Rev. E* **60**, 1063–1066 (1999).
- Snyder, J. *et al.* Low-temperature spin freezing in the $Dy_2Ti_2O_7$ spin ice. *Phys. Rev. B* **69**, 064414 (2004).
- Onsager, L. & Liu, C. T. Zur Theorie des Wieneffekts in schwachen Elektrolyten. *Z. Phys. Chem.* **228**, 428–432 (1965).
- Braunig, R., Gushimana, Y. & Ilgenfritz, G. Ionic-strength dependence of the electric dissociation field-effect—investigation of 2,6-dinitrophenol and application to the acid–alkaline transition of metmyoglobin and methemoglobin. *Biophys. Chem.* **26**, 181–191 (1987).
- Castelnovo, C., Moessner, R. & Sondhi, S. L. Thermal quenches in spin ice. *Phys. Rev. Lett.* **104**, 107201 (2010).
- Yavorskii, T., Fennell, T., Gingras, M. J. P. & Bramwell, S. T. $Dy_2Ti_2O_7$ spin ice: A test case for emergent clusters in a frustrated magnet. *Phys. Rev. Lett.* **101**, 037204 (2008).
- Fennell, T. *et al.* Neutron scattering studies of the spin ices $Ho_2Ti_2O_7$ and $Dy_2Ti_2O_7$ in applied magnetic field. *Phys. Rev. B* **72**, 224411 (2005).
- Orendáč, M. *et al.* Magnetocaloric study of spin relaxation in dipolar spin ice $Dy_2Ti_2O_7$. *Phys. Rev. B* **75**, 104425 (2007).
- Gledhill, J. A. & Patterson, A. A new method for measurement of the high field conductance of electrolytes (The Wien effect). *J. Phys. Chem.* **56**, 999–1005 (1952).
- Mydosh, J. A. *Spin Glasses: An Experimental Introduction* Ch. 3 (Taylor and Francis, 1993).

33. Lee, S-H. *et al.* Emergent excitations in a geometrically frustrated magnet. *Nature* **418**, 856–858 (2002).
34. Balents, L. Spin liquids in frustrated magnets. *Nature* **464**, 199–208 (2010).
35. Henley, C. L. The Coulomb phase in frustrated systems. *Annu. Rev. Condens. Matter Phys.* **1**, 179–210 (2010).
36. Wang, R. F. *et al.* Artificial 'spin ice' in a geometrically frustrated lattice of nanoscale ferromagnetic islands. *Nature* **439**, 303–306 (2006).
37. Ladak, S., Read, D. E., Perkins, G. K., Cohen, L. F. & Branford, W. R. Direct observation of magnetic monopole defects in an artificial spin-ice system. *Nature Phys.* **6**, 359–363 (2010).
38. Mengotti, E. *et al.* Real-space observation of emergent magnetic monopoles and associated Dirac strings in artificial kagome spin ice. *Nature Phys.* **7**, 68–74 (2011).
39. Weingärtner, H., Weiss, V. C. & Schröer, W. Ion association and electrical conductance minimum in Debye–Hückel-based theories of the hard sphere ionic fluid. *J. Chem. Phys.* **113**, 762–770 (2000).
40. Prabhakaran, D & Boothroyd, A. T. Crystal growth of spin-ice pyrochlores by the floating-zone method. *J. Cryst. Growth* doi:10.1016/j.jcrysgro.2010.11.049 (2010).

Acknowledgements

It is a pleasure to thank J. Dobson for technical assistance and the following for useful discussions: C. Castelnovo and R. Moessner (in particular for a correspondence concerning the Bjerrum volume), G. Aeppli, B. Kaas, T. Fennell, L. Jaubert and V. Kaiser. P.C.W.H. thanks the Max Planck Institute for Complex Systems, Dresden, for financial support.

Author contributions

The experimental work was carried out by S.R.G. and I.T., using a sample prepared by D.P. The analysis was carried out by S.T.B. and S.R.G. The theory was devised by S.T.B. and P.C.W.H. The manuscript was written by S.T.B., S.R.G. and P.C.W.H. with input and discussion from all authors.

Additional information

The authors declare no competing financial interests. Reprints and permissions information is available online at <http://npg.nature.com/reprintsandpermissions>. Correspondence and requests for materials should be addressed to S.R.G. or S.T.B.